DIELECTRIC CONSTANT MEASUREMENTS AT MICROWAVE FREQUENCIES

by

MERLIN EDWARD OLMSTEAD

B. S., Kansas State College
of Agriculture and Applied Science, 1947

A THESIS

submitted in partial fulfillment of the

requirements for the degree

MASTER OF SCIENCE

Department of Physics

KANSAS STATE COLLEGE
OF AGRICULTURE AND APPLIED SCIENCE

1949

TABLE OF CONTENTS

INTRODUCTION 1

THEORY 3

Electromagnetic Field Equations 3

Derivation of the Wave Equation 4

Solution of the Wave Equation 6

Development of Equations for TE_{01} Cylindrical Wave Guide. 11

Development of Equations for TE_{011} Cylindrical Cavity 14

Applications of Derived Equations to Dielectric Constant Measurements. 16

APPARATUS. 19

Microwave Generator 19

Wave Guide Attenuator 23

Cavity Wavemeter. 23

Test Cavity 26

Detector. 26

Amplifier 29

EXPERIMENTAL 33

Operation and Adjustments of the Reflex Klystron. 33

Wavemeter Calibration 37

Determination of the Modes of the Test Cavity 40

Method of Measuring Dielectric Constants. 42

Sample Computation. 45

SUMMARY AND DISCUSSION OF RESULTS. 47

ACKNOWLEDGMENTS. 49

LITERATURE CITED 50

INTRODUCTION

Methods of measuring dielectric constants of solids, liquids and gases have been known for many years. Recently there has been considerable development of methods of generating electromagnetic waves of ten centimeter wavelength and shorter. The development and application of these electromagnetic waves (microwaves) to communications and electrical measurements have led to the need for determining electrical constants at these wavelengths and at the same time have provided new tools by which these measurements may be made. The design of microwave apparatus, the propagation studies of microwave radiations, and applications in the newly developed field of microwave spectroscopy all require, in addition to other quantities, a knowledge of the dielectric constants of the materials concerned. In fact, the dielectric constant (as a symbol) occurs in almost all of the mathematical equations that describe the behavior of microwaves in wave guides and cavity resonators. The dielectric constants of many substances are constant over a wide range of wavelengths, while other substances may have considerable variation of this constant with wavelength. The measurements of dielectric constants with variation in wavelength, temperature and pressure which can now be extended to the microwave wavelengths should yield more information which can be used in studying the electrical and molecular properties of matter.

Of the various types of measurements utilizing microwave techniques (1, 2), the methods most often used are those involving measurements of the reflection of microwaves by the dielectric sample and those that involve the use of a cavity resonator. One type of measurement which

uses a reentrant cylindrical cavity involves a susceptance variation method (3) and requires calibration through empirical means. Another method using a cavity resonator (non-reentrant type) consists of the measurement of the change in the resonant length of the cavity due to the introduction of a sample of known thickness (4, 5, 6, 7).

The resonant cavity method of dielectric constant determination is limited in general to those substances that have low absorption at microwave frequencies. The introduction of the sample in the cavity causes the resonance curve of the cavity to become broad if the material has any appreciable absorption, and consequently the measurement of the shift in resonant length of the cavity becomes difficult to determine. With phenol type resins the absorption is so great that no resonance can be observed even with thin samples. A resonant cavity method which can be used with high loss materials or substances containing polar molecules uses only a small quantity of the material in the form of a small coaxial capillary (8) so that even though absorption is high the result on the cavity is small enough for a resonance to be obtained. The difficulty here is in measuring the small resonant shift accurately. Reflection methods (8, 9, 10, 11) involving the use of a standing wave detector (slotted line section of waveguide) may be used with samples having some absorption.

The cavity resonator method of dielectric constant measurements was chosen from among the various methods that could be used because the equipment required was more readily accessible than that required by other methods. Until recently this method had not been used as extensively by investigators in this country as other methods. It is particularly convenient where only thin samples of low loss samples are available and has

recently been used for measuring the dielectric constants of gases (6).

THEORY

In order to understand and develop the theory concerned with resonant cavities, it is necessary to start with the electromagnetic field equations rather than to attempt to explain the behavior of microwaves in terms of the concepts of low frequency systems. The method of the following theoretical development is to start with the electromagnetic field equations and to develop from them the relation that will yield the dielectric constant of a sample in terms of measurable quantities.

Electromagnetic Field Equations

Equation (1). Faraday's Law: $\nabla \times \underline{E} = -\frac{\partial \underline{B}}{\partial t}$

Equation (2). Ampere's Law: $\nabla \times \underline{H} = \underline{J} + \frac{\partial \underline{D}}{\partial t}$

Equation (3). Gauss's Law (electric field): $\nabla \cdot \underline{D} = \rho$

Equation (4). Gauss's Law (magnetic field): $\nabla \cdot \underline{B} = 0$

Equation (5). $\underline{D} = \mathcal{E} \underline{E}$)
Equation (6). $\underline{B} = \mu \underline{H}$) For homogeneous isotropic media

The conventional meaning of the symbols (M.K.S. system of units) are as follows:

$\underline{E}$ electric field intensity

$\underline{H}$ magnetic field intensity

$\underline{D}$ electric induction or flux density

$\underline{B}$ magnetic induction or flux density

$\underline{J}$ convection current density

ρ charge density

ε inductive capacity

μ permeability

Derivation of the Wave Equation

Only those waves which are sinusoidal functions of time and are propagated in a specified direction (say the z direction in a cylindrical coordinate system) will be considered since the generator of the electromagnetic waves is a sine wave oscillator.

$\underline{E}$ and $\underline{H}$ may be expressed by the equations

Equation (7). $\underline{E} = \underline{E}'(\phi,\rho)e^{j\omega t-\Gamma z}$

Equation (8). $\underline{H} = \underline{H}'(\phi,\rho)e^{j\omega t-\Gamma z}$

where $\underline{E}'$ and $\underline{H}'$ are the maximum electric and magnetic intensity respectively; $\omega = 2\pi f$ (f being the frequency of the generated wave in cycles per second); and $\Gamma = \alpha + j\beta$ is the propagation constant (α being the attenuation constant and β the phase factor).

From Equations (1) and (6): $\nabla \times \underline{E} = -\mu \frac{\partial \underline{H}}{\partial t}$

From Equations (2) and (5): $\nabla \times \underline{H} = \underline{J} + \varepsilon \frac{\partial \underline{E}}{\partial t} = \sigma \underline{E} + \varepsilon \frac{\partial \underline{E}}{\partial t}$

where σ is the conductivity of the medium.

By the use of these equations and Equations (7) and (8) the following equations are obtained:

Equation (9). $\nabla \times \underline{E} = -j\omega\mu \underline{H}$

Equation (10). $\nabla \times \underline{H} = (\sigma + j\omega\varepsilon)\underline{E}$

The following vector identity is true for any vector $\underline{A}$:

$$\nabla \times \nabla \times \underline{A} \equiv \nabla \nabla \cdot \underline{A} - \nabla^2 \underline{A}.$$

The curl of Equation (9) will give:

$$\nabla \times \nabla \times \underline{E} \equiv \nabla \nabla \cdot \underline{E} - \nabla^2 \underline{E} = -\nabla^2 \underline{E} \quad \text{because } \nabla \cdot \underline{E} = 0.$$

The curl of Equation (10) will give:

$$\nabla \times \nabla \times \underline{H} \equiv \nabla \nabla \cdot \underline{H} - \nabla^2 \underline{H} = -\nabla^2 \underline{H} \quad \text{since } \nabla \cdot \underline{H} = 0.$$

Then: $-\nabla^2 \underline{E} = -j\omega\mu(\nabla \times \underline{H}) = -j\omega\mu(\sigma + j\omega\varepsilon)\underline{E}$ and

$-\nabla^2 \underline{H} = (\sigma + j\omega\varepsilon)(\nabla \times \underline{E}) = (\sigma + j\omega\varepsilon)(-j\omega\mu)\underline{H}$.

For convenience in writing, $j\omega\mu(\sigma + j\omega\varepsilon)$ is set equal to a complex constant γ^2. The above equations then become:

Equation (11). $\nabla^2 \underline{E} = \gamma^2 \underline{E}$.

Equation (12). $\nabla^2 \underline{H} = \gamma^2 \underline{H}$.

The operation ∇^2 on a vector quantity $\underline{E}$ or $\underline{H}$ is considered as the operation of ∇^2 on the scalar components of $\underline{E}$ or $\underline{H}$.

The scalar component E_z of $\underline{E}$ operated upon by ∇^2 is written in cylindrical coordinates as:

Equation (13). $\frac{1}{\rho}\frac{\partial}{\partial\rho}\left(\rho\frac{\partial E_z}{\partial\rho}\right)+\frac{1}{\rho^2}\frac{\partial^2 E_z}{\partial\phi^2}+\frac{\partial^2 E_z}{\partial z^2}=\gamma^2 E_z$

where the coordinates are ρ, ϕ and z.

In Equations (7) and (8) $\underline{E}'$ and $\underline{H}'$ are functions of ρ and ϕ alone and

$$\frac{\partial^2 E_z}{\partial z^2}=\Gamma^2 E'_z \quad \text{by Equation (7).}$$

By the use of this relation Equation (13) can be rewritten in the form:

Equation (14). $\frac{1}{\rho}\frac{\partial}{\partial\rho}\left(\rho\frac{\partial E'_z}{\partial\rho}\right)+\frac{1}{\rho^2}\frac{\partial^2 E'_z}{\partial\phi^2}+\left(\Gamma^2-\gamma^2\right)E'_z e^{j\omega t-\Gamma z}=0.$

This partial differential equation is the wave equation of an electromagnetic wave propagated in the z direction and produced by a sine wave generator.

Solution of the Wave Equation

Equation (14) may be solved by separation of the variables. The solution is assumed to be of the form:

$$E'_z=R(\rho)\Phi(\phi)$$

where $R(\rho)$ is a function of ρ alone and $\Phi(\phi)$ is a function of ϕ alone.

Equation (14) can then be written in the form:

Equation (15). $R''\Phi+\frac{1}{\rho}R'\Phi+\frac{1}{\rho^2}R\Phi''+\left(\Gamma^2-\gamma^2\right)R\Phi=0.$

Multiplication by $\frac{\rho^2}{R\Phi}$ gives:

Equation (16). $\rho^2 \frac{R''}{R} + \rho \frac{R'}{R} + \left(\Gamma^2 - \gamma^2\right)\rho^2 = -\frac{\Phi''}{\Phi}$

Since the left side of this equation is a function of ρ alone, and the right side is a function of ϕ alone, the equation can be true for all values of ρ and ϕ only if each member is equal to a constant, say n^2.

Then: $-\frac{\Phi''}{\Phi} = n^2$

The solution of this ordinary differential equation is readily solved and can be written in the form:

Equation (17). $\Phi = C_1 \cos(n\phi) + C_2 \sin(n\phi)$ (since $n^2 > 0$)

where C_1 and C_2 are arbitrary constants.

$$\rho^2 \frac{R''}{R} + \rho \frac{R'}{R} + \left(\Gamma^2 - \gamma^2\right)\rho^2 = n^2$$

can be rewritten in the form

Equation (18). $\rho^2 R'' + \rho R' + \left[\left(\Gamma^2 - \gamma^2\right)\rho^2 - n^2\right] R = 0.$

Equation (18) is an ordinary differential equation involving the independent variable ρ.

A change of variable $u = \sqrt{\Gamma^2 - \gamma^2}$ transforms this equation into the following form:

Equation (19). $u^2 \frac{d^2R}{du^2} + u \frac{dR}{du} + \left(u^2 - n^2\right)R = 0.$

This ordinary differential equation is recognizable as Bessel's differential equation and can be solved by series methods (12, 13).

The general solution of Equation (19) may be written as:

Equation (20). $R(\rho) = C_3 J_n(u) + C_4 K_n(u)$

where C_3 and C_4 are arbitrary constants and

$$J_n(u) = \sum_{m=0} \frac{(-1)^m \left(\frac{u}{2}\right)^{n+2m}}{m!\,(m+n)!}$$

$$K_n(u) = \frac{J_n(u) \cos n\pi - J_{-n}(u)}{\sin n\pi} .$$

$J_n(u)$ is the Bessel function of the first kind and of order n. $K_n(u)$ is the Bessel function of the second kind and of order n.

$E_z = E' e^{j\omega t - \Gamma z} = R(\rho)\Phi(\phi) e^{j\omega t - \Gamma z}$ becomes:

Equation (21). $E_z = \left[C_3 J_n(u) + C_4 K_n(u)\right] \left[C_1 \cos n\phi + C_2 \sin n\phi\right] e^{j\omega t - \Gamma z}$.

By following exactly the same procedure with H_z as was used for E_z, the solution for H_z may be written:

Equation (22). $H_z = \left[C_7 J_n(u) + C_8 K_n(u)\right] \left[C_5 \cos n\phi + C_6 \sin n\phi\right] e^{j\omega t - \Gamma z}$.

Since $u = \sqrt{\Gamma^2 - \gamma^2}\,\rho$, $K_n(u)$ becomes infinite for $\rho = 0$.

The solution desired will involve finite axial fields which can only be obtained by setting C_4 and C_8 equal to zero. The desired solution will also be applied to wave guides or cavities with cylindrical symmetry and hence it is only necessary to retain either a cosine or sine variation of E_z or H_z with ϕ.

The cosine term will be retained and C_2 and C_6 are set equal to zero. C_1C_3 is set equal to a constant E_{0z} and C_5C_7 is set equal to H_{0z}.

Under these considerations, Equations (21) and (22) reduce to:

Equation (23). $E_z = E_{0z}J_n(u)\cos(n\phi)e^{j\omega t-\Gamma z}$.

Equation (24). $H_z = H_{0z}J_n(u)\cos(n\phi)e^{j\omega t-\Gamma z}$.

The type of resonant cavity which is ordinarily used in dielectric constant measurements is of the $TE_{01\ell}$ mode, where ℓ is any integer greater than zero. This means that there will be no longitudinal component of $\underline{E}$ and hence $E_z = 0$.

The left members of Equations (9) and (10) are written in cylindrical coordinates, and the components are equated to the corresponding components of the right-hand members.

Equation (25). $\Gamma E_\phi = -j\omega\mu H_\rho$.

Equation (26). $-\Gamma E_\rho = -j\omega\mu H_\phi$.

Equation (27). $\frac{1}{\rho}\frac{\partial(\rho E_\phi)}{\partial\rho} - \frac{1}{\rho}\frac{\partial E_\rho}{\partial\phi} = -j\omega\mu H_z$.

Equation (28). $\frac{1}{\rho}\frac{\partial H_z}{\partial\phi} + \Gamma H_\phi = (\sigma + j\omega\varepsilon)E_\rho$.

Equation (29). $-\Gamma H_\rho - \frac{\partial H_z}{\partial\rho} = (\sigma + j\omega\varepsilon)E_\phi$.

Equation (30). $\frac{\partial(\rho H_\phi)}{\partial\rho} = \frac{\partial H_\rho}{\partial\phi}$.

Equation (25) gives: $-\frac{E_\phi}{H_\rho} = \frac{j\omega\mu}{\Gamma}$

Equation (26) gives: $\frac{E_\rho}{H_\phi} = \frac{j\omega\mu}{\Gamma}$.

Then $\frac{E_\rho}{H_\phi} = -\frac{E_\phi}{H_\rho}$.

Equation (28) may now be rewritten in the form:

$$\frac{1}{\rho}\frac{\partial H_z}{\partial \phi} + H_\phi\left[\Gamma - \frac{j\omega\mu}{\Gamma}(\epsilon + j\omega\ell)\right] = 0, \text{ or}$$

$$H_\phi = -\frac{\Gamma}{(\Gamma^2 - \gamma^2)\rho}\frac{\partial H_z}{\partial \phi}$$

Substitution of the value of H_z given by Equation (24) gives

$$H_\phi = \frac{\Gamma\ (n)}{(\Gamma^2 - \gamma^2)\rho} H_{Oz} J_n(u) \sin(n\phi) e^{j\omega t - \Gamma z}.$$

Equation (29) can be solved for H_ρ as follows:

$$-\Gamma H_\rho - \frac{\partial H_z}{\partial \rho} + \frac{(\epsilon + j\omega\ell)j\omega\mu H}{\Gamma} = 0$$

$$\frac{\Gamma^2 - \gamma^2}{\Gamma} H_\rho = -\frac{\partial H_z}{\partial \rho}$$

$$H_\rho = -\frac{\Gamma}{\Gamma^2 - \gamma^2}\frac{\partial H_z}{\partial \rho}$$

$$H_\rho = -\Gamma\sqrt{\Gamma^2 - \gamma^2}\, J_n'(u) \cos(n\phi) e^{j\omega t - \Gamma z}$$

$$H_\rho = -\frac{\Gamma\rho}{\sqrt{\Gamma^2 - \gamma^2}} H_{Oz} J_n'(u) \cos(n\phi) e^{j\omega t - \Gamma z}$$

The six field components may now be written down.

Equation (31). $$H_\rho = -\frac{\Gamma}{\sqrt{\Gamma^2 - \gamma^2}} H_{0s} J_n'\left(\sqrt{\Gamma^2 - \gamma^2}\,\rho\right) \cos(n\phi) e^{j\omega t - \Gamma z}.$$

Equation (32). $$H_\phi = \frac{\Gamma n}{\left(\Gamma^2 - \gamma^2\right)} H_{0s} J_n\left(\sqrt{\Gamma^2 - \gamma^2}\,\rho\right) \sin(n\phi) e^{j\omega t - \Gamma z}.$$

Equation (33). $$H_z = H_{0s} J_n\left(\sqrt{\Gamma^2 - \gamma^2}\,\rho\right) \cos(n\phi) e^{j\omega t - \Gamma z}.$$

Equation (34). $$E_\rho = \frac{j\omega\mu}{\Gamma} H_\phi$$

Equation (35). $$E_\phi = -\frac{j\omega\mu}{\Gamma} H_\rho = \frac{j\omega\mu}{\sqrt{\Gamma^2 - \gamma^2}} H_{0s} J_n'\left(\sqrt{\Gamma^2 - \gamma^2}\,\rho\right) \cos(n\phi) e^{j\omega t - \Gamma z}.$$

Equation (36). $E_z = 0.$

Development of Equations for TE_{01} Cylindrical Wave Guide

At the wave guide wall where $\rho = b$ = radius of cylinder, E_ϕ must be zero since there can exist no tangential component of $\underline{E}$ in the conductor. H_ρ must also be zero for $\rho = b$ since $E_\phi = 0$ under this condition.

Then: $J_n'\left(\sqrt{\Gamma^2 - \gamma^2}\, b\right) = 0.$

Let $\sqrt{\Gamma^2 - \gamma^2}\, b = M$, where M represents the roots of $J'(x) = 0$.

Then:

Equation (37). $$\sqrt{\Gamma^2 - \gamma^2} = \frac{M}{b} \quad \text{or}$$

Equation (38). $\Gamma^2 = \left(\frac{\pi}{b}\right)^2 + \gamma^2$

Since $\Gamma = \alpha + j\beta$ and

$$\gamma = \sqrt{j\omega\mu(\sigma + j\omega\varepsilon)}$$

Equation (38) may be rewritten as:

$$\alpha^2 - \beta^2 + 2j\alpha\beta = \left(\frac{\pi}{b}\right)^2 + j\omega\mu\sigma - \omega^2\mu\varepsilon \cdot$$

The real parts of this equation are equated and the attenuation constant is neglected since it is usually very small. This gives:

$$-\beta^2 = \frac{\pi}{b}^2 - \omega^2\mu\varepsilon \quad \text{or}$$

Equation (39). $\beta^2 = \omega^2\mu\varepsilon - \left(\frac{\pi}{b}\right)^2$

If $\omega^2\mu\varepsilon > \left(\frac{\pi}{b}\right)^2$, $j\beta$ will be imaginary and waves will be propagated through the guide or cavity. If $\omega^2\mu\varepsilon < \left(\frac{\pi}{b}\right)^2$, $j\beta$ will be real and waves will not be propagated. The cut-off occurs when $\left(\frac{\pi}{b}\right)^2 - \omega_c^2\mu\varepsilon = 0$, where ω_c is the angular frequency that satisfies this relation.

Then:

Equation (40). $\left(\frac{\pi}{b}\right)^2 - \omega_c^2 = \frac{4\pi^2}{\lambda_c^2}$

where $f_c = \frac{1}{\lambda_c\sqrt{\mu\varepsilon}}$ is the cut-off frequency and λ_c is the cut-off wavelength.

Equation (41). $\omega^2\mu\epsilon = \frac{4\pi^2\mu_g\epsilon_g}{\lambda^2} = \beta^2 + \frac{4\pi^2}{\lambda_c^2}$

where $f = \frac{1}{\lambda\sqrt{\mu_0\epsilon_0}}$ is the frequency of the propagated wave, λ is the free space wavelength of the wave being propagated, $\mu_g = \frac{\mu}{\mu_0}$ and $\epsilon_g = \frac{\epsilon}{\epsilon_0}$.

Equation (42). $\beta^2 = \omega^2\mu\epsilon = \frac{4\pi^2}{\lambda_g^2}$

where λ_g is the wavelength of the propagated wave in the guide.

Substitution of Equation (42) in Equation (41) and dividing by $4\pi^2$ gives:

Equation (43). $\frac{\mu_g\epsilon_g}{\lambda^2} \quad \frac{1}{\lambda_g^2} \quad \frac{1}{\lambda_c^2}$

From Equation (40) the value of λ_c may be obtained as

$$\lambda_c = \frac{\pi d}{M}$$

where $d = 2b$ is the diameter of the guide or cavity and M represents the roots of $J_n'(x) = 0$.

With operation in the TE_{01} type mode, there should be no variation of fields with ϕ. This requires that n equal zero in the equation for the field components. With n set equal to zero, H_ϕ and E_ρ vanish and $J_0'(x)$ replaces $J_n'(x)$.

Using the relations $\sqrt{\Gamma^2 - \gamma^2} = \frac{M}{b} = \frac{2\pi}{\lambda_c}$ and (neglecting α)

$\Gamma = j\beta = j\frac{2\pi}{\lambda_g}$, the equation for TE_{01} waves becomes:

Equation (44). $H_\rho = -j\frac{\lambda_c}{\lambda_g} H_{0z} J_0'\left(\frac{2\pi\rho}{\lambda_c}\right) e^{j\left(\omega t - \frac{2\pi}{\lambda_g} z\right)}$.

Equation (45). $H_z = H_{0z} J_0\left(\frac{2\pi\rho}{\lambda_c}\right) e^{j\left(\omega t - \frac{2\pi}{\lambda_g} z\right)}$.

Equation (46). $E_\phi = -\frac{j\omega\mu\lambda_c}{2\pi} H_{0z} J_0'\left(\frac{2\pi\rho}{\lambda_c}\right) e^{j\left(\omega t - \frac{2\pi}{\lambda_g} z\right)}$

Development of Equations for TE_{011} Cylindrical Cavity

If the propagated wave is reflected by a perfect conductor placed across the guide, say at $z = 0$, then the sum of the incident and reflected waves at $z = 0$ must give for E_ϕ a zero resultant since no tangential component of E may exist in a perfect conductor. The condition which must be satisfied at $z = 0$ is:

Equation (47). $\frac{-j\omega\mu\lambda_c}{2\pi} H_{0z} J_0'\left(\frac{2\pi\rho}{\lambda_c}\right) e^{j\omega t}\left[e^{-j\left(\frac{2\pi}{\lambda_g} z\right)} + e^{j\left(\frac{2\pi}{\lambda_g} z + \Psi\right)}\right] = 0.$

where Ψ is the phase relation between the incident and reflected value of E_ϕ which is to be determined by this equation.

Equation (47) is satisfied if $1 + e^{j\Psi} = 0$

or $\Psi = (2k + 1)\pi$

where k is any integer.

$e^{-j\left(\frac{2\pi}{\lambda_g} z\right)} + e^{j\left(\frac{2\pi}{\lambda_g} z + \Psi\right)}$ becomes:

$e^{-j\left(\frac{2\pi}{\lambda_g} z\right)} - e^{j\left(\frac{2\pi}{\lambda_g} z\right)}$ and is true for all z since the phase factor determines the relative phase of the reflected and incident waves not only at the boundary, but throughout the entire guide or cavity.

The roots of $e^{-j\left(\frac{2\pi}{\lambda_g} z\right)} - e^{j\left(\frac{2\pi}{\lambda_g} z\right)} = 0$ occur when

$$\frac{2}{\lambda_g} z = m, \quad m = 0, 1, 2, \ldots .$$

For $m = 1$, $z = \frac{\lambda_g}{2}$, which indicates that the smallest cavity length which will satisfy the boundary conditions necessary for standing waves is $z = \frac{\lambda_g}{2}$. With resonant length $z = \frac{\lambda_g}{2}$, the cavity mode is called a TE_{011} type mode.

Since the sine of any angle θ can be written in the form:

$$\sin\theta = \frac{1}{2}\left(e^{-j\theta} - e^{j\theta}\right),$$

the resultant E_ϕ can be written:

Equation (48). $E_\phi = -\frac{\omega\mu\lambda_c}{\pi} H_{0z} J_1'\left(\frac{2\pi}{\lambda_c}\rho\right) e^{j\omega t} \sin\frac{2\pi}{\lambda_g} z$.

Equation (9) gives: $H_\rho = \frac{-1}{\omega\mu}\frac{\partial E_\phi}{\partial z}$ or

Equation (49). $H_\rho = j\frac{2\lambda_c}{\lambda_g} H_{0z} J_0'\left(\frac{2\pi\rho}{\lambda_c}\right) e^{j\omega t} \cos\frac{2\pi}{\lambda_g} z$.

Equation (10) with δ neglected gives:

$$\frac{\partial H_\rho}{\partial z} - \frac{\partial H_z}{\partial \rho} = (6 + j\omega\epsilon)E_\phi = j\omega\epsilon E_\phi$$

$$\frac{\partial H_z}{\partial \rho} = \frac{\partial H_\rho}{\partial z} - j\omega\epsilon E_\phi$$

H_z can be obtained by performing the indicated operations.

$$\frac{2\pi}{\lambda_c} H_z \frac{J_0'\left(\frac{2\pi\rho}{\lambda_c}\right)}{J_0\left(\frac{2\pi\rho}{\lambda_c}\right)} = -j\left[\frac{4\pi\lambda_c}{\lambda_g^2} - \frac{\omega^2\mu\epsilon\lambda_c}{\pi}\right] H_{0z} J_0\left(\frac{2\pi\rho}{\lambda_c}\right) e^{j\omega t} \sin\frac{2\pi}{\lambda_g} z .$$

$$H_z = -j\frac{\lambda_c}{2\pi}\left[4\pi\frac{\lambda_c}{\lambda_g^2} - 4\pi\left(\frac{\lambda_c}{\lambda_g^2} + \frac{\lambda_c}{\lambda_c^2}\right)\right] H_{0z} J_0\left(\frac{2\pi\rho}{\lambda_c}\right) e^{j\omega t} \sin\frac{2\pi}{\lambda_g} z .$$

This reduces to:

Equation (50). $H_z = -2jH_{0z} J_0' \frac{2\pi\rho}{\lambda_c} e^{j\omega t} \sin\frac{2\pi}{\lambda_g} z .$

Equations (48), (49), and (50) are the equations for a TE_{011} cavity resonator.

Applications of Derived Equations to Dielectric Constant Measurements

At the boundary surface between two dielectrics (1 and 2), the tangential components of the electric and magnetic fields are equal.

$$E_{t_1} = E_{t_2} \text{ and } H_{t_1} = H_{t_2}$$

If the boundary surface is free of charges, the normal components of the electric intensity and magnetic intensity are equal.

$$\varepsilon_1 E_{n_1} = \varepsilon_2 E_{n_2} \text{ and } \mu_1 H_{n_1} = \mu_2 H_{n_2}$$

There will also be reflections occurring at the boundary of two dielectrics, but these reflections will not meet the required boundary conditions at the end of the cavity and will be absorbed by the cavity. The reflected waves will cause out-of-phase currents in the end walls of the cavity which will result in nearly complete attenuation of these waves. The energy is lost in the form of heat in the cavity end walls. These reflections will result in a slight lowering of the Q of the cavity because of the absorption but will have practically no effect on the resonant frequency change of the cavity due to the introduction of a dielectric sample in the cavity. The dielectric sample is placed in the cavity as shown in the following diagram:

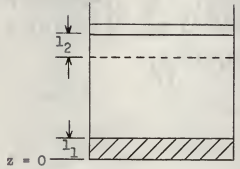

l_1 is the thickness of the dielectric sample.

l_2 is the reduction in resonant length of the cavity due to the introduction of the dielectric.

The path length in air is decreased by a distance $l_1 + l_2$. Since the total equivalent path length in air must remain unchanged, the path length in the dielectric must be equivalent to a path length of $l_1 + l_2$ in air. This means that a path length of l_1 in the dielectric is equivalent to a path length of $l_1 + l_2$ in air. Then if $z \leq l_1$, the path length of z in the dielectric is equivalent to a path length of $z + l_2$ in air.

From Equations (48), (49), and (50), the equations in the dielectric may be written:

Equation (51). $$E_{\phi d} = -\frac{A\omega\mu_d\lambda_c}{\pi} H_{0s} J'_0\left(\frac{2\pi\rho}{\lambda_c}\right) e^{j\omega t} \sin\frac{2\pi}{\lambda_d} z$$

Equation (52). $$H_{\rho d} = jA\frac{2\lambda_c}{\lambda_d} H_{0s} J'_0\left(\frac{2\pi\rho}{\lambda_c}\right) e^{j\omega t} \cos\frac{2\pi}{\lambda_d} z$$

Equation (53). $$H_{zd} = -jA2H_{0s} J_0\left(\frac{2\pi\rho}{\lambda_c}\right) e^{j\omega t} \sin\frac{2\pi}{\lambda_d} z$$

where A indicates an attenuation in the dielectric and z may be less than or equal to l_1.

The equations in air in the cavity may be written:

Equation (54). $$E_{\phi a} = -\frac{\omega\mu_a\lambda_c}{\pi} H_{0s} J'_0\left(\frac{2\pi\rho}{\lambda_c}\right) e^{j\omega t} \sin\left[\frac{2\pi}{\lambda_a}(z + l_2)\right]$$

Equation (55). $$H_{\rho a} = j\frac{2\lambda_c}{\lambda_a} H_{0s} J'_0\left(\frac{2\pi\rho}{\lambda_c}\right) e^{j\omega t} \cos\left[\frac{2\pi}{\lambda_a}(z + l_2)\right]$$

Equation (56). $$H_{za} = -j2H_{0s} J_0\left(\frac{2\pi\rho}{\lambda_c}\right) e^{j\omega t} \sin\left[\frac{2\pi}{\lambda_a}(z + l_2)\right]$$

By the boundary conditions:

$$E_{\phi a} = E_{\phi d}$$
$$H_{\rho a} = H_{\rho d} \qquad \text{at } z = l_1$$

Equations (51) and (54) give:

$$\mu_a \sin\left[\frac{2\pi}{\lambda_a}(l_1 + l_2)\right] = \mu_d \sin \frac{2\pi}{\lambda_d} l_1$$

Equations (52) and (55) give:

$$\frac{1}{\lambda_a} \cos\left[\frac{2\pi}{\lambda_a}(l_1 + l_2)\right] = \frac{A}{\lambda_d} \cos \frac{2\pi}{\lambda_d} l_1$$

Thence $\mu_a \lambda_a \tan\left[\frac{2\pi}{\lambda_a}(l_1 + l_2)\right] = \mu_d \lambda_d \tan \frac{2\pi}{\lambda_d} l_1$

In general μ_a will be equal to μ_d, so that the desired relation may be written in the form:

Equation (57). $\lambda_a \tan\left[\frac{2\pi}{\lambda_a}(l_1 + l_2)\right] = \lambda_d \tan \frac{2\pi}{\lambda_d} l_1$

Equation (43) may be used to determine λ_a.

λ_d may then be determined by Equation (57). The dielectric constant of the sample is then given by Equation (43) as:

$$\varepsilon_d = \lambda^2 \left(\frac{1}{\lambda_d^2} + \frac{1}{\lambda_c^2}\right)$$

λ_c is determined by equation: $\lambda_c = \frac{\pi d}{M}$ by Equation (40).

APPARATUS

Microwave Generator

The source of microwave energy was furnished by a reflex klystron oscillator operating in the three centimeter wavelength region. The type

of klystron was 723 A/B with adjustable frequency of from approximately 8700 to 9700 megacycles per second. Microwave energy was removed from the klystron by means of a coaxial line projecting from the base of the tube. The reflex klystron was mounted on a short section of wave guide so that the coaxial line of the klystron projected through a hole in the center of the broad edge of the guide. This enabled microwave energy to be propagated down the guide.

The frequency output of the reflex klystron may be varied by varying the voltage applied to the repeller plate. The magnitude and rate of change of the frequency of the klystron depend on the type of klystron, the magnitude of the repeller voltage and the frequency and waveform of the modulating voltage. In addition to the modulating voltage a fixed bias voltage must be applied to the repeller plate of the klystron in order to obtain a resultant voltage which will be of the proper value.

The source of the modulating voltage that was used was that of the saw-tooth oscillator of a Dumont type 208-B oscilloscope. The bias supply was furnished by a ninety-volt battery. The battery supply was necessary because the available regulated power supplies were not sufficiently well regulated to keep the average frequency of the klystron constant. The method that was used to connect the saw-tooth voltage and modulating voltage to the klystron is shown in Plate I. A diode restorer was used to keep the base level of the negative saw-tooth voltage at the value of the bias voltage. The two potentiometers were used to permit adjustments of the base level and the amplitude of the saw-tooth voltage applied to the repeller plate. The frequency of the saw-tooth voltage was varied by the frequency control on the oscilloscope. A 300 volt regulated power supply was used for the accelerat-

EXPLANATION OF PLATE I

Schematic diagram of the microwave generator showing the method of application of voltage.

C_1, C_2	1 Mfd., 600 v. condenser.
R_1	120,000 ohm resistor.
R_2	20,000 ohm potentiometer.
R_3	100,000 ohm potentiometer.
V_1	723 A/B reflex klystron.
V_2	6H6 diode.

PLATE I

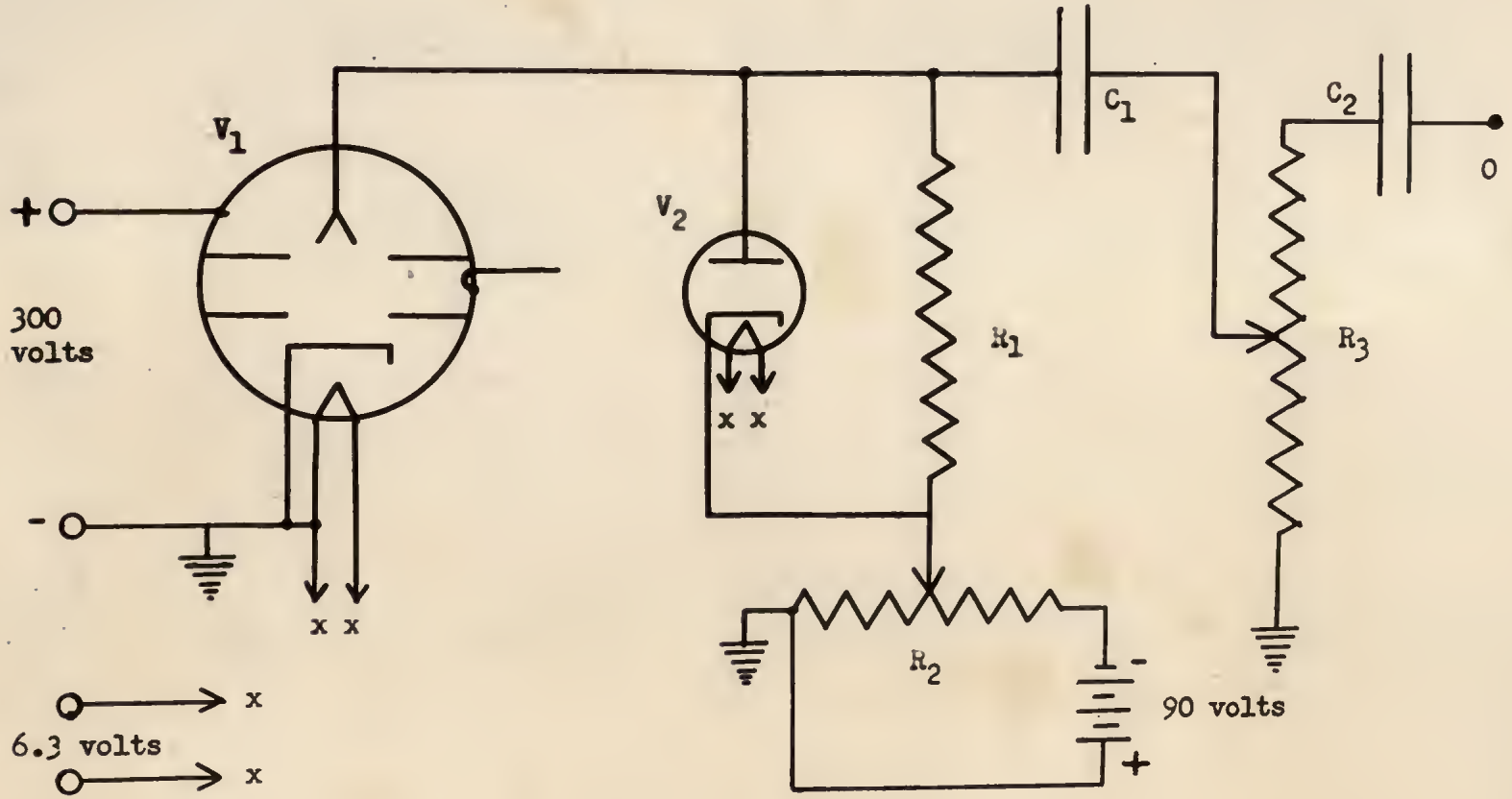

ing voltage of the klystron. Slight variations of the voltage of this supply did not appear to have any effect on the average frequency output of the klystron.

Wave Guide Attenuator

An attenuator consists of a short section of wave guide containing lossy material which will absorb part of the energy which passes through it. The type of attenuator that was used consisted of a metalized glass strip mounted parallel to the narrow side of the guide and made adjustable in position relative to the side and center of the guide. The electric field is a maximum in the center of the guide and zero at the side of the guide. Maximum attenuation results when the metalized strip is in the center of the guide, and minimum attenuation is obtained when the strip is at the side. The variations observed with the attenuator used were from practically no attenuation to complete attenuation.

Cavity Wavemeter

The cavity wavemeter that was used was a transmission type cylindrical TE_{011} three centimeter General Electronic Industries wavemeter. The construction is the same as that shown in Fig. 1, Plate II. Only the frequency to which the cavity is set will be transmitted through the wavemeter. A calibration curve giving the transmission frequency corresponding to micrometer settings is necessary for use as a wavemeter. Calibration of the wavemeter will be described later.

EXPLANATION OF PLATE II

Fig. 1 Drawing of the transmission type cavity wavemeter.

Fig. 2 Schematic diagrams showing the method used in calibrating a 1N23A type crystal.

PLATE II

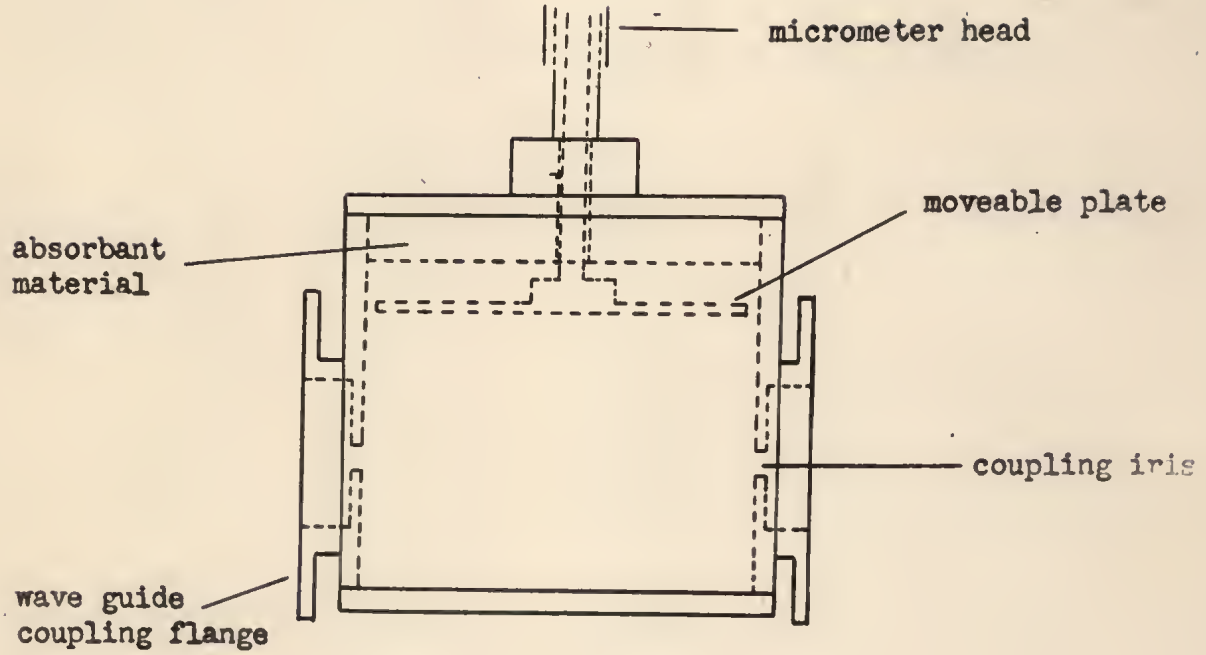

Figure 1.

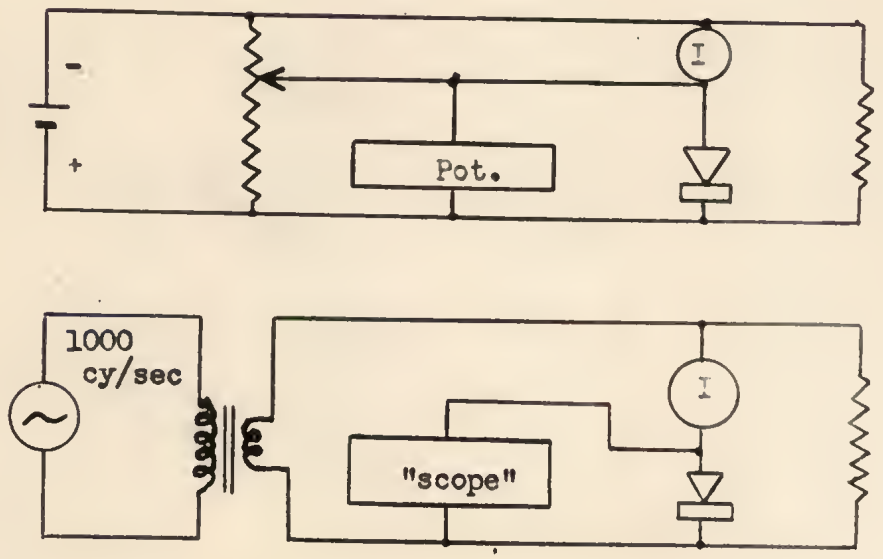

Figure 2.

Test Cavity

The three centimeter TE_{011} cavity that was used for dielectric constant measurements is called the test cavity. Figure 1, Plate II, shows the construction, which is exactly the same as the construction of the wavemeter described above. The top and bottom plates were removed and the bottom plate was replaced with shellac added to the parts where the plate and cylinder make contact. This was done in order to make the cavity leak proof to liquids that were introduced into the cavity for dielectric determinations. The top plate was left unfastened so that dielectric samples could be introduced and removed quickly. The method used to determine the modes present in the test cavity will be described later.

Detector

The detector consisted of a type 1N23A standard microwave crystal detector mounted in a detecting section. The detecting section is a short section of wave guide closed at one end and holding the crystal. The crystal is placed in the center of the guide parallel to the electric field. Measurements were made with one type of crystal to determine the characteristics of rectification. It was desirable to know the operating region over which the "square law" of detection is obeyed. The arrangement of apparatus using a load resistance of twenty ohms is shown in Fig. 2, Plate II. The results of direct current measurement are shown in Figs. 3 and 4. In Fig. 3, I_c is the forward crystal current, while I_c' is the reverse current. Figure 4 shows the range of crystal current over

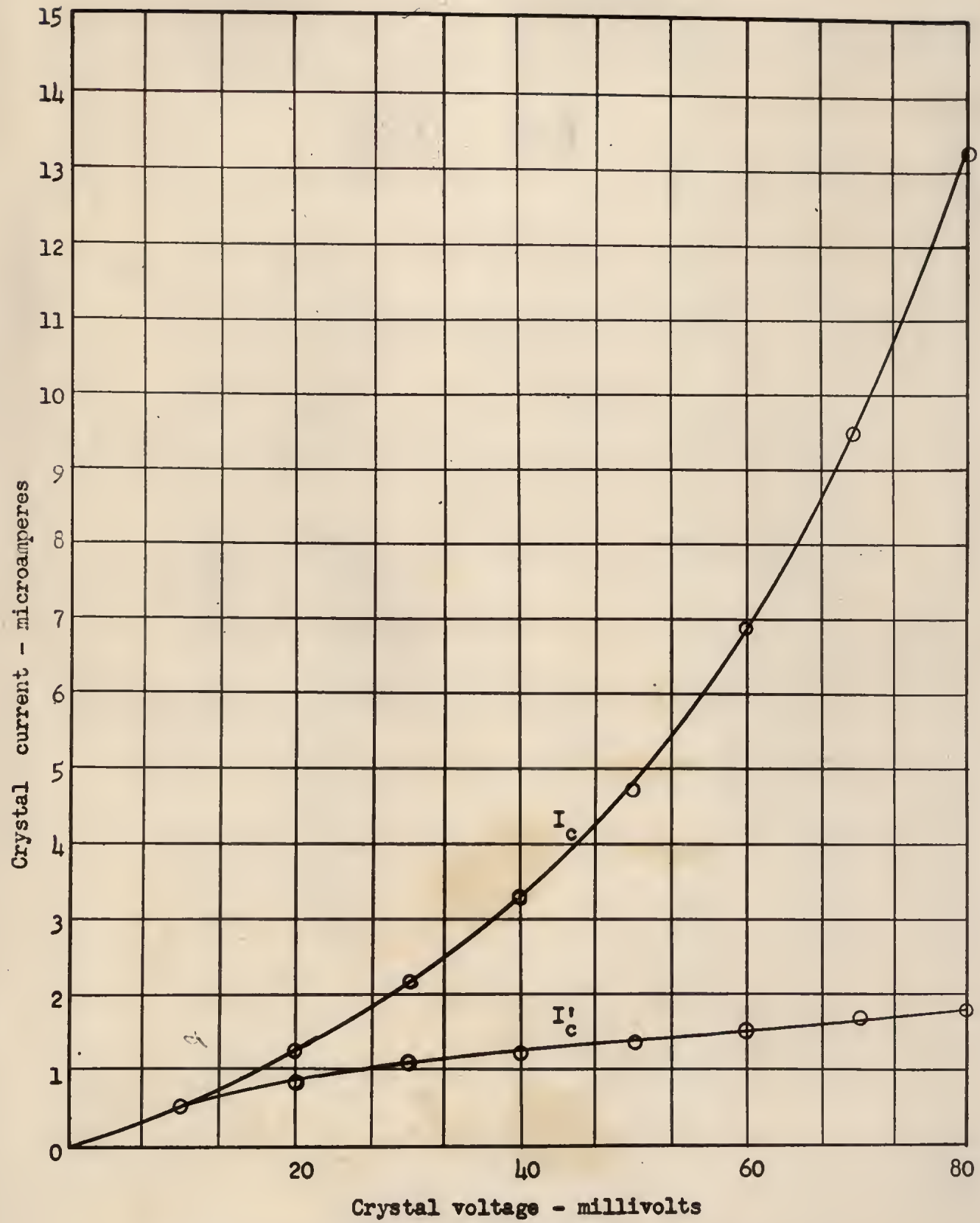

Figure 3. Rectification characteristic of 1N23A Crystal.

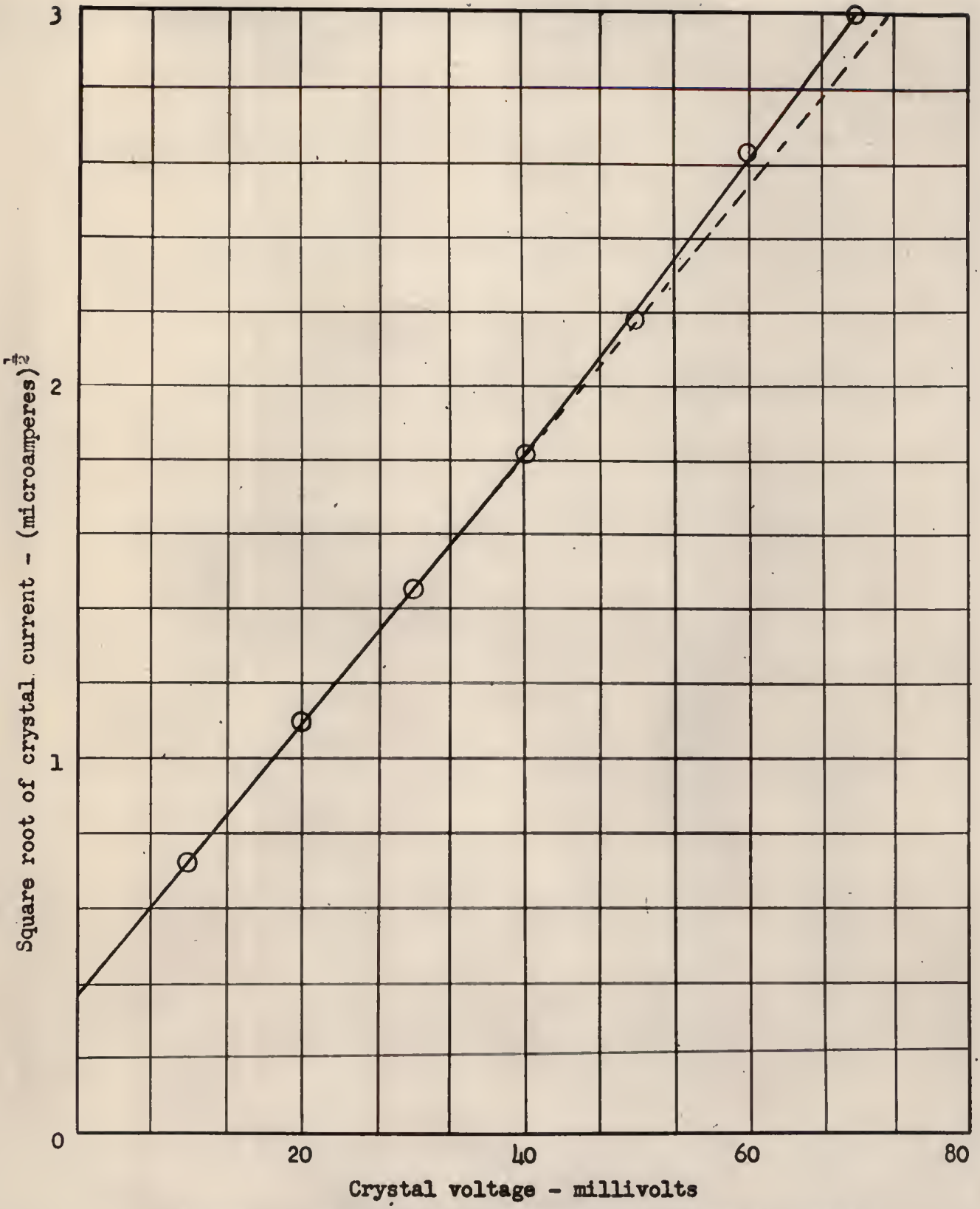

Figure 4. Rectification characteristic of 1N23A crystal.

which the "square law" detection is obeyed. Figure 5 shows the result of measurements made of the detection at 1000 cycles per second. Curve A, Fig. 5, shows the range of currents over which "square law" detection is obeyed.

Amplifier

The energy obtained through rectification of the microwaves used in dielectric constant measurements was extremely small. It was found necessary to construct an amplifier to amplify the rectified voltage from the crystal detector in order to operate the indicator (oscilloscope). The amplifiers that were available contained too much 60 cycle voltage in the output to be of use. Plate III shows the schematic diagram of the amplifier. Shielding was used on the input, output, and high voltage supply leads. The coupling condensers between stages were rather small at first (about .001 Mfd.) but were later increased somewhat because only sharply peaked wave forms were being amplified to any extent. The tubes used were all type 6AC7's. The circuit is that of a conventional three-stage resistance-capacitance coupled amplifier. A stabilized 300 volt power supply was used for the plate supply and a 6.3 volt, 60 cycle source for the heater supply. There was no noticeable increase in 60 cycle output by the use of the alternating current heater supply in place of a direct current supply. The only fault that could be found with the amplifier was the microphonic action of the 6AC7 vacuum tubes.

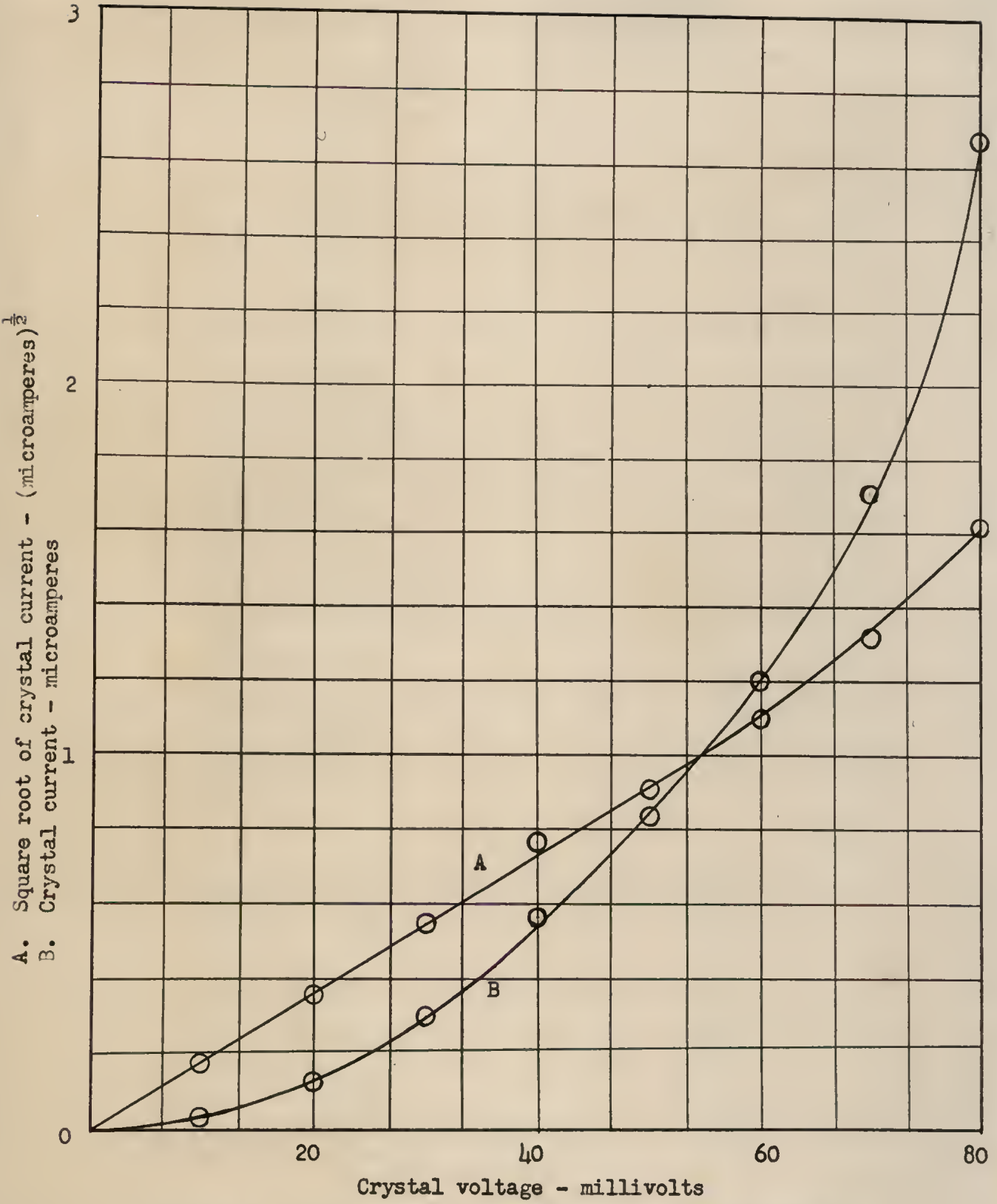

Figure 5. Rectification characteristic of 1N23A crystal at 1000 cycles per second.

EXPLANATION OF PLATE III

Schematic diagram of the amplifier that was built for use in microwave measurements.

C_1, C_3, C_7, C_{11}, C_{13}	.05 Mfd., 400 v. condensers.
C_2, C_6, C_{10}	50 Mfd., 150 v. condensers.
C_4, C_8, C_{12}	.1 Mfd., 600 v. condensers.
C_5	.01 Mfd., 600 v. condenser.
C_9	.04 Mfd., 600 v. condenser.
R_1, R_6, R_{11}	.5 megohm condenser.
R_2, R_3, R_7, R_8, R_{13}, R_{14}	68,000 ohm resistor.
R_4, R_9, R_{15}	1500 ohm resistor.
R_5, R_{10}, R_{12}	150 ohm resistor.

PLATE III

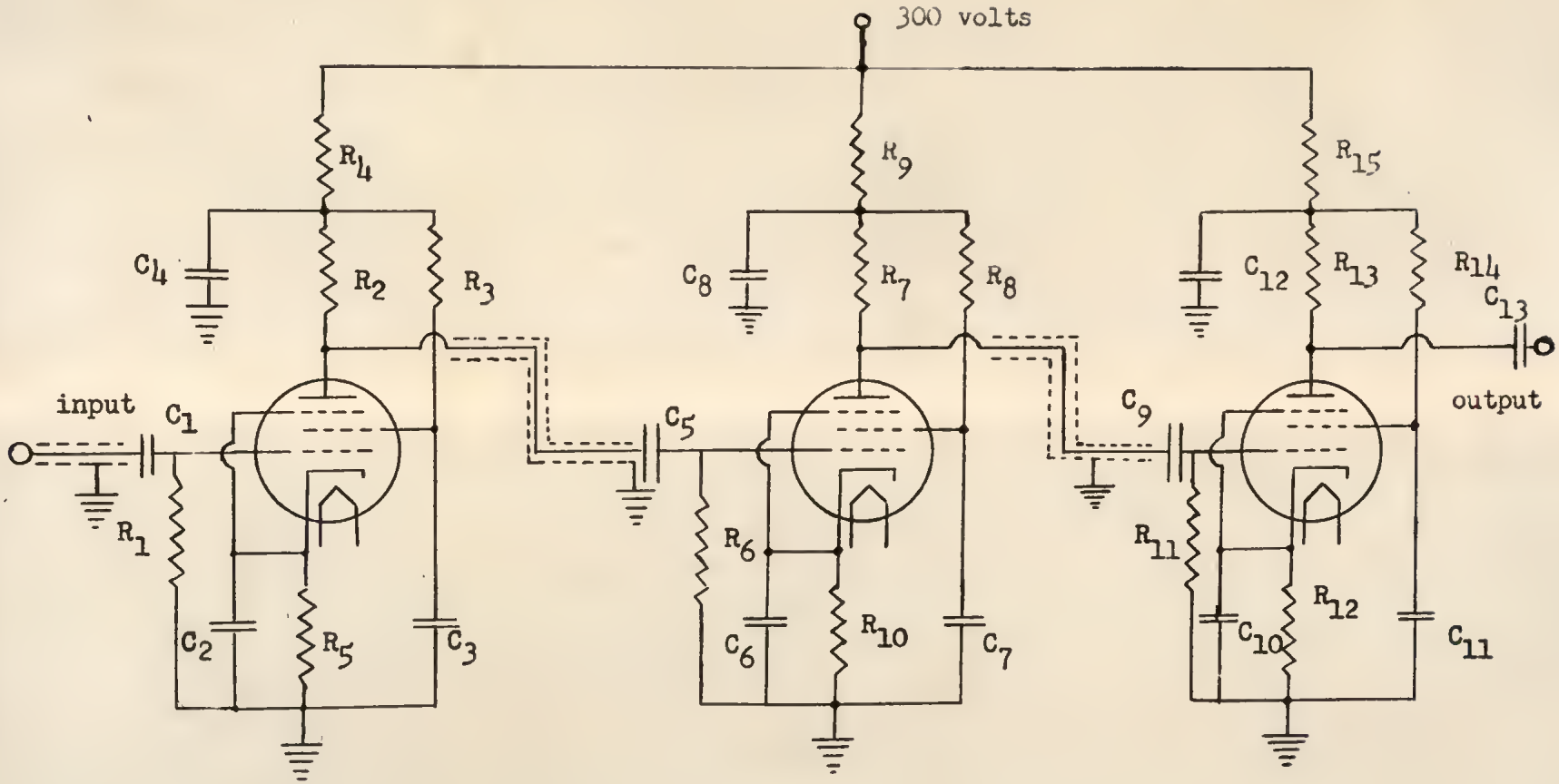
300 volts
R4
R9
R15
C4
R2
R3
C8
R7
R8
C12
R13
R14
C13
input
C1
C5
C9
output
R1
R6
R11
C2
R5
C3
C6
R10
C7
R12
C10
C11

EXPERIMENTAL

Operation and Adjustments of the Reflex Klystron

The frequency output of the reflex klystron is determined by a mechanical adjustment and an electrical adjustment. The mechanical adjustment of the frequency of the reflex klystron of the type used is accomplished by turning a set screw which changes the grid spacing in the tube. The electrical adjustment of the frequency is accomplished by varying the magnitude of the negative voltage applied to the repeller plate. The type of variations of power output and frequency with repeller plate (or reflector) voltage is shown in Fig. 6, Plate IV. The maximum output is obtained at the frequency determined by the mechanical adjustment. The range of reflector voltage which gives an output is called a voltage mode of operation. Figure 6, Plate IV, shows three voltage modes of operation. When the output of the reflex klystron is passed through a waveguide to a crystal detector and the rectified signal passed through a microammeter, indication of output is given by deflections of the microammeter as the repeller voltage is varied.

Figure 7, Plate IV, shows the type of variation of the frequency and output of the reflex klystron with time as the reflector voltage is varied by a saw-tooth wave voltage superimposed upon the direct current reflector voltage. The method of applying the direct current and saw-tooth voltages is shown in Plate I. The saw-tooth voltage obtained from an oscilloscope is connected to the terminal marked O and to ground. The saw-tooth modulation results in both frequency and amplitude modulation of the output of the

EXPLANATION OF PLATE IV

Fig. 6 Typical variation of power output and frequency of a reflex klystron with reflector voltage.

Fig. 7 Saw-tooth frequency modulation of a reflex klystron.

PLATE IV

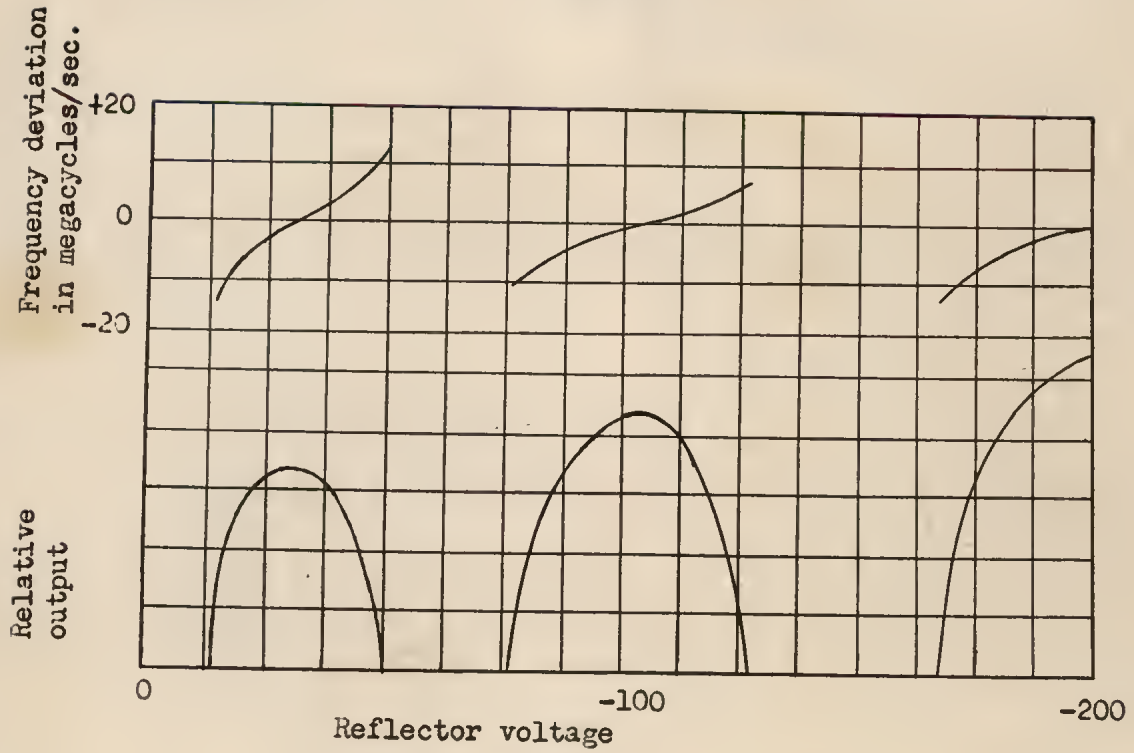

Figure 6.

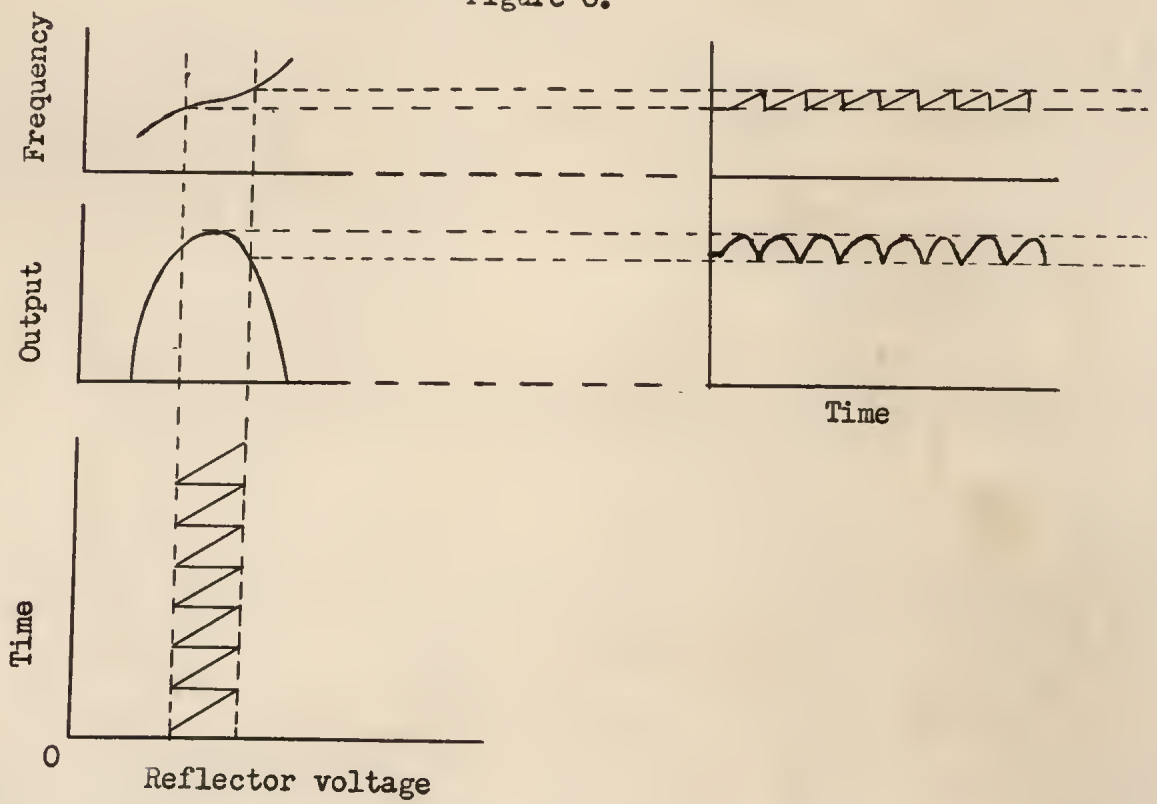

Figure 7.

reflex klystron and, therefore, permits the use of an amplifier to amplify the rectified output from the detector. The amplified signal is applied to the vertical amplifier of an oscilloscope, while the saw-tooth voltage is applied to the horizontal amplifier. The resulting pattern on the screen of the oscilloscope is essentially a visual graph of output (vertically) against frequency (horizontally).

The procedure that was used was to adjust the potentiometer R_3 (see Plate I) for maximum saw-tooth modulation and then to adjust the set screw on the reflex klystron until an output at the desired frequency was obtained. The resulting pattern on the screen had an appearance very similar to the power output vs. reflector voltage curve of Fig. 6, Plate IV. The magnitude of the saw-tooth voltage may then be reduced and R_2 varied at the same time so that the output curve remains on the oscilloscope screen. The resulting pattern on the screen now has an appearance similar to that of one of the humps of the output vs. time curve of Fig. 7, Plate IV. The position of this pattern on the oscilloscope screen can be shifted to the right or to the left by varying the setting of the potentiometer R_2. The hump of the pattern may be spread out or flattened by still further reduction of the saw-tooth modulation voltage. Various modulation frequencies can be used according to the setting of the frequency control of the oscilloscope.

Since the pattern obtained on the oscilloscope screen is a visual graph of output against frequency, any absorption of microwave energy at one of the frequencies represented on the horizontal axis of the oscilloscope screen will result in a sharp dip of the curve at the position on the screen corresponding to that frequency. If the frequency absorbed were

to vary, the dip in the curve would appear to move across the oscilloscope screen. Absorption wavemeters absorb an extremely narrow band of frequencies about the frequency to which they are set and produce an effect exactly as described above when inserted between the microwave source and detector. If the wavemeter is calibrated, the frequency of the "pip" on the screen will be known.

Wavemeter Calibration

It was necessary to calibrate a transmission type wavemeter before it could be used as a reference cavity in dielectric constant measurements. A reaction type calibrated wavemeter covering the desired range of frequencies was used for the calibration. A coaxial cable ending in a probe was used to couple the microwave energy into the wavemeter. The arrangement of the apparatus is shown in Fig. 8, Plate V.

The reflex klystron was adjusted until an output was obtained which resulted in a broad humped curve on the oscilloscope screen. The height of the hump was varied by the gain control of the horizontal amplifier of the oscilloscope and by the setting of the attenuator. The attenuator was always adjusted for the maximum attenuation that would still give sufficient output. This was done to give the maximum isolation between the oscillator and the wavemeter in order that there would be minimum reaction on the oscillator frequency due to the wavemeters. The calibrated wavemeter was adjusted until an absorption pip appeared on the oscilloscope screen. The transmission type wavemeter was adjusted until another absorption pip appeared on the screen. The position of this pip was varied until it

EXPLANATION OF PLATE V

Fig. 8 Block diagram showing arrangement of apparatus for use in the calibration of a resonant cavity wavemeter.

Fig. 9 Block diagram showing arrangement of apparatus for use in dielectric constant determinations.

LEGEND

A . . . . . Oscilloscope.
B . . . . . Microwave generator.
C . . . . . Wave guide attenuator.
D . . . . . Probe.
E . . . . . Wavemeter to be calibrated.
F . . . . . Coaxial line.
G . . . . . Calibrated wavemeter and detector.
H . . . . . Amplifier.
I . . . . . Test cavity.
J . . . . . Detector.

PLATE V

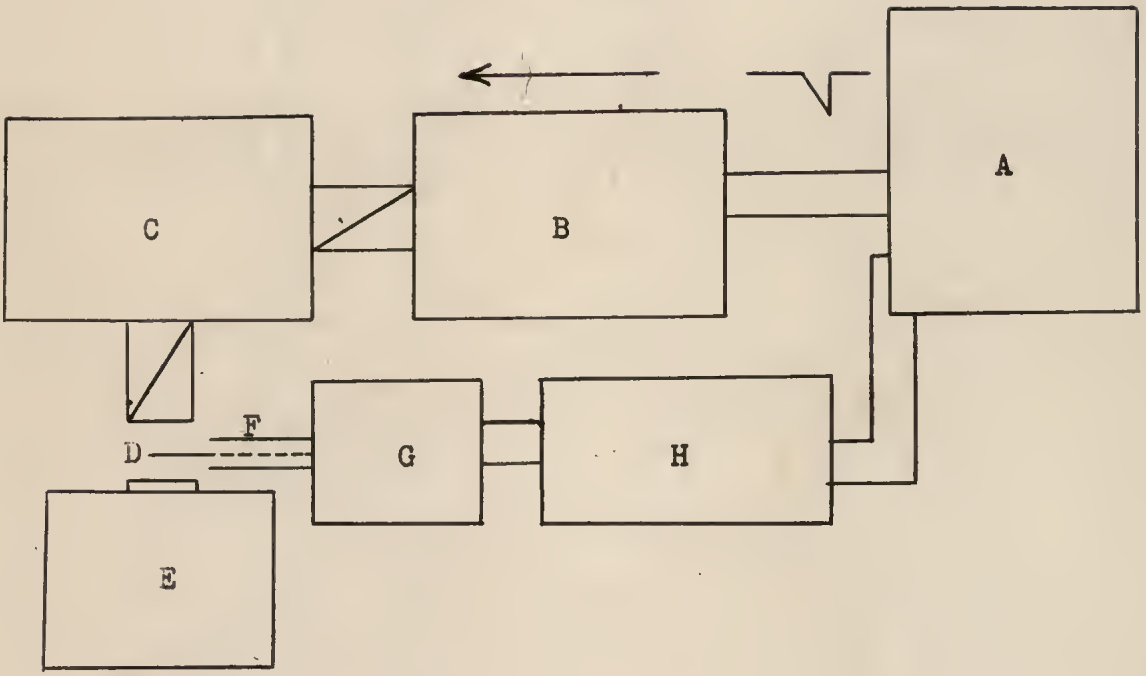

Figure 8.

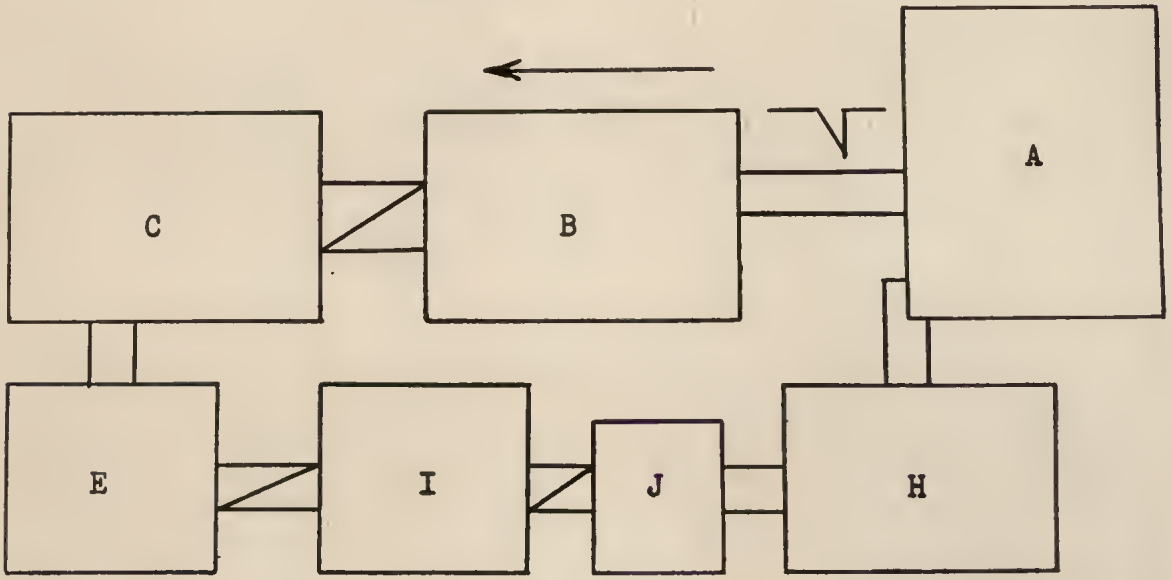

Figure 9.

coincided with that due to the calibrated wavemeter. When this is done, the two wavemeters are resonant at exactly the same frequency. The micrometer setting of the transmission type wavemeter was recorded, together with the frequency of the calibrated wavemeter corresponding to its micrometer reading. The frequency of the reflex klystron was then changed and the above procedure repeated. This was done throughout the entire range of frequencies covered by the calibrated wavemeter. A graph of the frequency against micrometer setting was plotted, thereby giving the calibration desired.

Determination of the Modes of the Test Cavity

In order to determine whether the transmission type cavity (that was available) could be used for dielectric constant measurements, it was necessary to determine the number and type of modes present. Calibration by means of a calibrated reaction type wavemeter resulted in a calibration curve which is shown in Fig. 10. This graph indicated that there were three modes of operation. The center curve is that of the fundamental mode and resonances due to this mode were very much stronger and sharper than those due to the other two.

To determine the type of modes represented by the three curves, a measurement of the inside diameter of the cavity and a measurement of the length of the cavity corresponding to a micrometer setting was necessary. From this second measurement the resonant wavelength in air in the cavity for a given frequency (and micrometer setting) could be determined. This measured wavelength differed from the actual wavelength by a small value

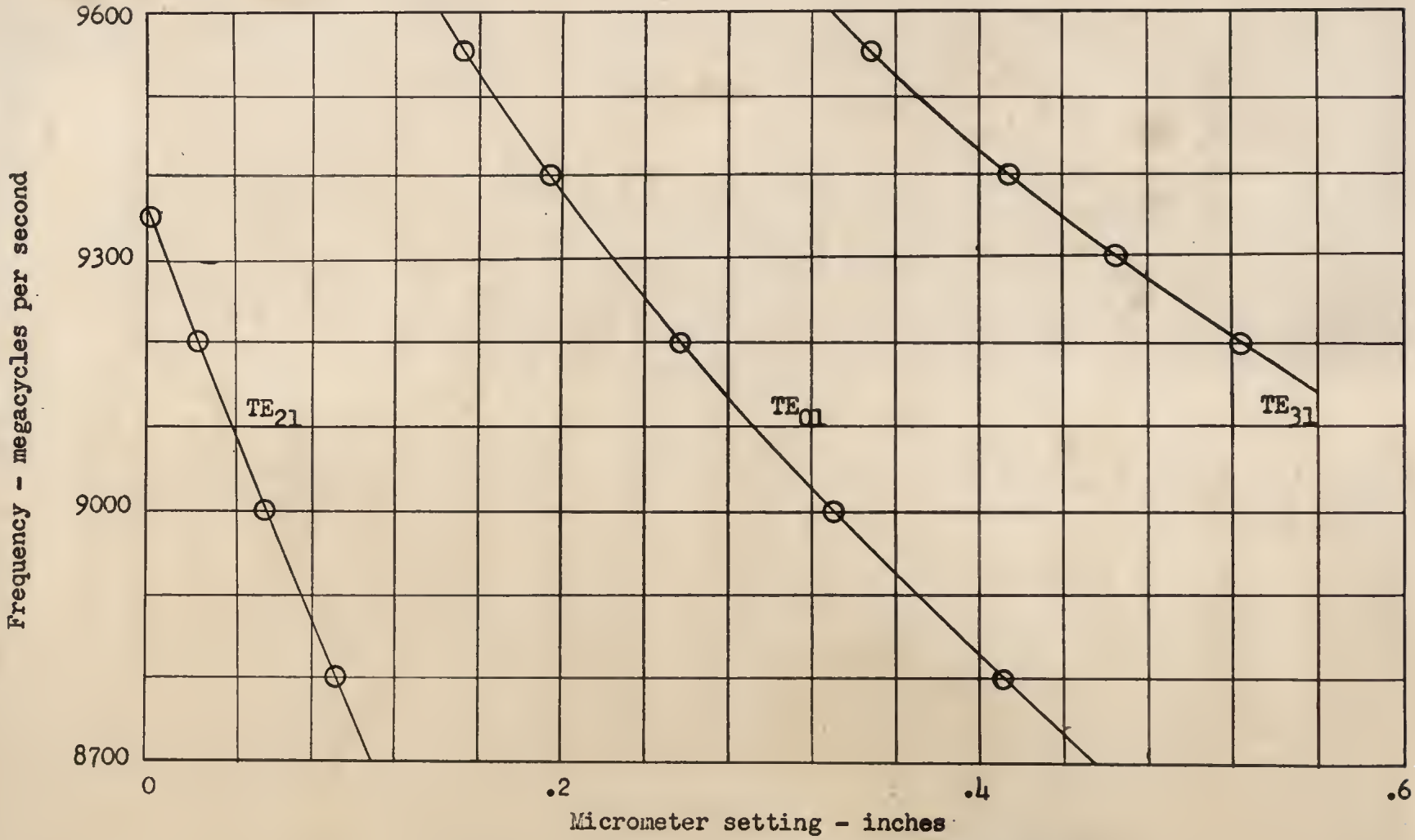

Figure 10. Test cavity (type TE_{01}) calibration.

but was accurate enough to permit determinations of the modes. The cut-off wavelength was calculated by the use of Equation (43), page 13. The value of $\frac{M}{\pi}$ was calculated from $\lambda_c = \frac{\pi d}{M}$. This value of $\frac{M}{\pi}$, when compared with those given in Table 1, determined the mode. The values given in Table 1 are calculated by dividing the roots of the Bessel functions of the first kind of order M by .

An examination of the calibration graph giving the positions of the two weak modes and the strong TE_{011} mode indicated that the cavity could be used for dielectric constant measurements, although the accuracy to be expected would not be as good as that attained by a cavity especially designed for dielectric constant measurements.

Method of Measuring Dielectric Constants

The arrangement of the apparatus used for dielectric constant measurements is shown in Fig. 9, Plate V. The calibrated reference cavity allowed only the frequency to which it is set to pass through to the test cavity. If the test cavity is not resonant to the same frequency as the reference cavity, no energy can pass through it to the detector and the pattern on the oscilloscope screen will merely be a straight horizontal line. If the two resonant cavities are resonant to the same frequency and the reflex klystron "sweeps" over this frequency, there will be a vertical line (extremely sharp resonant curve) on the oscilloscope screen. The test cavity is carefully adjusted for maximum height of this vertical line. The two cavities are now resonant at exactly the same frequency.

Table 1. Values of $\frac{M}{\pi}$.

	H_{nm} TE_{nm} Modes		
n m =	1	2	3
0	1.2197	2.2331	3.238
1	0.5861	1.6970	2.7172
2	0.9721	2.134	3.172
3	1.3373	2.5513	
4	1.6926	2.9547	
5	2.0421		
6	2.3877		

	E_{nm} TM_{nm} Modes		
n m =	1	2	3
0	0.7655	1.7571	2.7546
1	1.2197	2.2331	3.238
2	1.6347	2.6793	3.6988
3	2.0309	3.1070	
4	2.4154		
5	2.7920		
6	3.1628		

The setting of the micrometer spindle of the test cavity can be reproduced to an accuracy of plus or minus one ten thousandths of an inch by watching the oscilloscope screen and adjusting for maximum height of the vertical line. This accuracy is about as good as the micrometer setting can be read, since the ten thousandths place is estimated.

The dielectric sample was prepared in the form of a thin disc with a diameter slightly less than the inside diameter of the cavity. In most cases the plates from which the discs were cut were not accurately flat, and it was necessary to surface each face of the plate to insure constant thickness of the discs. The surfacing operation, which was accomplished by use of a lathe, was not entirely satisfactory, however, since variations in thickness of nearly a thousandths of an inch still remained.

The test cavity was removed and the calibrated reference cavity was set to the frequency desired for a dielectric constant measurement. The reflex klystron was adjusted until a vertical line (indicating output) was obtained on the oscilloscope screen. The test cavity was replaced and adjusted until an output was again obtained. The test cavity was carefully adjusted for maximum height of the line on the oscilloscope screen and the micrometer reading was recorded. The dielectric sample was then placed in the bottom of the test cavity and the micrometer spindle readjusted (cavity length must be reduced) until output was again obtained. The micrometer reading was again recorded. The dielectric sample was removed and its average thickness measured. The resonant frequency of the resonant cavity was noted. The data obtained by these operations, together with a knowledge of the cut-off wavelength of the cavity, enabled the dielectric constant of the sample to be determined.

Dielectric measurements of transformer oil and liquid petroleum were measured by the same method as described above. The thickness of the liquid layer was measured by use of a travelling microscope. Precautions were taken to insure that the cavity was level during the dielectric constant measurements. The travelling microscope did not prove to be very satisfactory because of the inability of the eye to determine the exact position of focus with the desired precision.

Sample Computation

The following is an example of the method of calculating the dielectric constant of a sample from the data obtained:

Polystyrene Sample.

Data:

Test Cavity diameter (d)	4.948 cm.
$\frac{M}{\pi}$ for TE_{011} cavity	1.2197
Dielectric constant of air (ϵ_a)	1.00059
Resonant frequency of reference cavity (f)	8900 mc/sec.
Thickness of sample (l_1)	0.4059 cm.
Test cavity micrometer setting (empty cavity)	0.3652 inch
Test cavity micrometer setting (cavity with sample).	0.2952 inch

Calculations:

Cut-off wavelength $\lambda_c = \frac{\pi d}{M} = \frac{4.948}{1.2197} = 4.057$ cm.

Free-space wavelength $\lambda = \frac{c}{f} = \frac{29977.6}{8900} = 3.368$ cm.

Reduction in resonant length of test cavity $l_2 = (.3652 - .2952) \times 2.54$ cm.

$$l_1 = 0.1778 \text{ cm.}$$

$$\lambda_a = \frac{1}{\sqrt{\frac{\epsilon_a}{\lambda^2} - \frac{1}{\lambda_c^2}}} = 6.039 \text{ cm.}$$

$$\frac{\lambda_a}{2\pi l_1} \tan \frac{2\pi(l_1 + l_2)}{\lambda_a} = \frac{\lambda_d}{2\pi l_1} \tan \frac{2\pi l_1}{\lambda_d}$$

$$\frac{6.039}{2\pi \times .4059} \tan \frac{2\pi \times 0.5837}{6.039} = \frac{\tan \theta}{\theta}$$

where $\theta = \frac{2\pi l_1}{\lambda_d}$

$$\frac{\tan \theta}{\theta} = 1.646$$

The value of θ may be obtained from a graph obtained by plotting $\frac{\tan \theta}{\theta}$ against θ for values of $\frac{\tan \theta}{\theta}$ near the value given.

$$\theta = 1.042$$

$$\lambda_d = \frac{2\pi l_1}{\theta} = \frac{2\pi \times .4059}{1.042} = 2.448 \text{ cm.}$$

$$\epsilon_d = \lambda^2 \left(\frac{1}{\lambda_d^2} + \frac{1}{\lambda_c^2}\right) = 11.34(.1669 + .06076)$$

$$\epsilon_d = 2.58$$

SUMMARY AND DISCUSSION OF RESULTS

The results of dielectric constant measurements on polystyrene, plexiglass, transformer oil, liquid petroleum and a glass sample are shown in Table 2. The values obtained for the solid samples are more consistent than those obtained for the liquid samples. The chief cause of the variations in the results for the liquid samples is due to the inaccuracies in the measurement of the thickness of the liquid.

The values of the dielectric constant for plexiglass and polystyrene fall within the values obtained by other investigators using similar and different methods. The average value of the dielectric constant obtained for transformer oil is very nearly the square of the index of refraction of this oil. More measurements are required to determine the dielectric constant of liquid petroleum.

The results obtained indicate that dielectric constants of low loss dielectrics may be determined with an accuracy of several per cent by the use of the apparatus and methods described. Greater accuracy could be obtained with liquid specimens by increasing the accuracy of measuring depths of liquids in a cavity.

The method of measuring dielectric constants that was used is not new in principle, but it differs in the use of a frequency modulated source instead of a fixed stabilized oscillator. The method appears to be as accurate as those using the fixed frequency source and, in addition, provides a visual indication of the absorption due to the dielectric.

Table 2. Results of dielectric constant measurements.

Sample thickness (centimeters)	Frequency of measurement (megacycles per second)	Dielectric constant
	Polystyrene	
.4059	8900	2.58
.4059	9200	2.56
.2667	8900	2.63
.2667	9200	2.64
.4720	9050	2.56
	Glass sample	
.2324	9350	7.54
	Plexiglass	
.3289	9050	2.71
.4318	9050	2.68
	Transformer oil	
.147	9200	2.28
.255	9200	2.13
.332	9200	2.24
.384	9200	2.24
.449	9200	2.26
.685	9200	1.82
	Liquid petroleum	
.186	9200	2.48
.424	9200	2.23
.450	9200	1.88
.623	9200	1.46

ACKNOWLEDGMENTS

Acknowledgment is gratefully made to Dr. L. D. Ellsworth for his valuable aid and suggestions, and to Professor E. V. Floyd for construction of part of the experimental equipment.

LITERATURE CITED

(1) Montgomery, C. G.
Technique of microwave measurements. New York: McGraw-Hill, 1947. pp. 561-666.

(2) Jackson, Willis.
The representation of dielectric properties and the principles underlying their measurement at centimetre wavelengths. Trans. Farad. Soc. 42A:91-101. 1946.

(3) Works, C. N.
Resonant cavities for dielectric measurements. Jour. Appl. Phys. 18:605-12. 1947.

(4) Penrose, R. P.
Some measurements of the permittivity and power factor of low loss solids at 25,000 mc/sec. frequency. Trans. Farad. Soc. 42A:108-114. 1946.

(5) Bleaney, J., H. N. Loubser, and R. P. Penrose.
Cavity resonators for measurements with centimetre electromagnetic waves. Proc. Phys. Soc. (London). 59:185-199. 1947.

(6) Jen, C. K.
A method for measuring the complex dielectric constant of gases at microwave frequencies by using a resonant cavity. Jour. Appl. Phys. 19:649-53. 1948.

(7) Lamb, J.
Measurements of the dielectric properties of ice. Trans. Farad. Soc. 42A:238-44. 1946.

(8) Surber, W. H., Jr.
Universal curves for dielectric-filled wave guides and microwave dielectric measurement methods for liquids. Jour. Appl. Phys. 19:514-23. 1948.

(9) Surber, W. H., Jr., and C. E. Crouch, Jr.
Dielectric measurement methods for solids at microwave frequencies. Jour. Appl. Phys. 19:1130-39. 1948.

(10) Roberts, S., and A. von Hippel.
New method for measuring dielectric constant and loss in the range of centimeter waves. Jour. Appl. Phys. 17:610. 1946.

(11) Dakin, T. W., and C. N. Works.
Microwave dielectric measurements. Jour. Appl. Phys. 18:789. 1947.

(12) Churchill, R. V.
Fourier series and boundary value problems. New York: McGraw-Hill, 1941. pp. 143-47.

(13) Forsyth, A. R.
A treatise on differential equations. London: Macmillan, 1943. Chap. V.